DOI: 10.17344/acsi.2025.9607 *Acta Chim. Slov.* **2026,** *73,* 54–61

Scientific paper

Study of thermal decomposition of $(Ba_{0.7}Ca_{0.3})TiO_3$ and $Ba(Zr_{0.2}Ti_{0.8})O_3$ xerogels and thin films

Sabi William Konsago,[1,2,*] Dean Birmančević,[1] Jena Cilenšek,[1] Brigita Kmet,[1,2] Katarina Žiberna,[1,2] Barbara Malič[1,2,*]

[1] *Jožef Stefan Institute, Jamova cesta 39, 1000 Ljubljana, Slovenia*

[2] *Jožef Stefan International Postgraduate School, Jamova cesta 39, 1000 Ljubljana, Slovenia*

* *Corresponding author: E-mail: sabi.william.konsago@ijs.si, Barbara.Malic@ijs.si*

Received: 11-08-2025

Dedicated to the memory of Prof. Dr. Boris Žemva

Abstract

Understanding the thermal decomposition and perovskite phase crystallization enables the design of the desired microstructure of $BaTiO_3$-based thin films prepared by chemical solution deposition. We prepared xerogels from $(Ba_{0.7}Ca_{0.3})TiO_3$ (BCT) and $Ba(Zr_{0.2}Ti_{0.8})O_3$ (BZT) coating solutions, as well as BCT and BZT thin films, to investigate their thermal decomposition. The oxycarbonates, formed during the heating of BCT and BZT xerogels, are fully decomposed at 780 °C and 720 °C, respectively. The thermal decomposition of carbonate residues in BCT and BZT thin films is completed at 750 °C and 700 °C, respectively. The approximately 120 nm thick BCT and BZT films annealed at 850 °C crystallize in the perovskite phase.

Keywords: $Ba(Zr_{0.2}Ti_{0.8})O_3$, $(Ba_{0.7}Ca_{0.3})TiO_3$, thin films, thermal analysis, FTIR, thermal decomposition

1. Introduction

Barium titanate ($BaTiO_3$, BT) is a prototype ferroelectric material, one of the most studied dielectric materials in bulk ceramic, multilayer, thick or thin film forms. Essentially used as capacitors in the radar systems during the Second World War, BT and its derivatives, nowadays, are used for various applications, including microelectromechanical systems (MEMS) such as actuators, sensors, dynamic and non-volatile ferroelectric random-access memories (DRAM and FeRAM), energy storage, etc.[1–3] In the latter applications, the active materials are mainly used in their thin film forms.

Chemical solution deposition (CSD) of thin films enables chemical modification and control of stoichiometry in thin-film processing, allowing control over the materials' chemical composition and homogeneity.[4] The physical properties of functional oxide thin films, such as BT and its derivatives, depend on their chemical composition, defects, and microstructure. These parameters can be controlled by understanding the solution chemistry and the chemistry at each processing stage to achieve the desired microstructural features and functional properties of the oxide thin films. Hoffman et al. prepared $SrTiO_3$ and BT thin films on platinized silicon substrates consisting of columnar grains by decreasing the concentration of the coating solution to 0.1 M and by multistep annealing at 800 °C, i.e., by repeating the solution deposition, drying, pyrolysis, and annealing steps until the required thickness was achieved.[5] Note that the standard procedure for BT coating solution preparation involves carboxylic acid and 2-methoxyethanol solvents, the latter of which is toxic to humans and the environment.[6] In our earlier work, BT thin films with a columnar microstructure were prepared at 800 °C using a coating solution with a two times higher concentration (0.2 M) and employing ethylene glycol and ethanol as solvents for Ba-acetate and Ti-butoxide, respectively. This combination of solvents increased the stability of the coating solution. The decomposition temperature of the organic residues in BT thin films was about 600 °C, which is almost 100 °C lower than in the conventional acetic acid-alcohol-based route.[7]

In 2009, it was reported that an equimolar solid solution of tetragonal Ca-modified BT and rhombohedral Zr-modified BT, $0.5Ba(Zr_{0.2}Ti_{0.8})O_3–0.5(Ba_{0.7}Ca_{0.3})TiO_3$, denoted BZT–BCT, resulted in a bulk ceramic material

with extraordinarily high piezoelectric properties, making it a potential lead-free alternative to lead-based piezoelectric ceramics.[8] Phase relations in the BT–$CaTiO_3$ (CT)–$BaZrO_3$ (BZ) system were studied as early as the 1950s.[9] A limited solid solubility of CT in BT was observed (up to about 25 mol % CT), while the BZ–BT solid solution was stable within the whole compositional range. The Curie temperature of BT–CT within its solid solubility range remains almost the same, at about 130 °C, while in the BZ-BT solid solution it decreases with increasing BZ content, reaching room temperature at slightly above 20 mol % BZ. BT–CT exhibits dielectric and ferroelectric properties that are lower than in BT, while BT–BZ exhibits a ferroelectric-relaxor crossover at about 20 mol % BZ.[10–12] There are only a few reports of functional properties in BCT and BZT thin films, and with limited or nonexisting microstructural details.[13–16] For example, it has been reported that the relaxor-like properties of $Ba(Zr_xTi_{1-x})O_3$ with $x \geq 0.2$ make it a promising material for energy storage applications.[17]

The good ferroelectric and piezoelectric properties of BZT–BCT make it a suitable lead-free candidate for MEMS or energy harvesting applications, where the active material is in a cantilever form.[8, 18,19] However, BZT–BCT thin films with a granular and porous microstructure were obtained following the conventional BT film processing conditions. To achieve the columnar thin films, the BZT–BCT coating solution was diluted to 0.1 M, and the annealing temperature was increased to 850 °C.[4,20] The observed differences between BT and BZT–BCT films could only be explained by the changes in solution chemistry, which influence the thermal decomposition and consequent perovskite crystallization pathways resulting from the addition of Ca-acetate or Ti-butoxide to the BT coating solution, or by the combination of both. In the study, the thermal decomposition of $Ba_{0.7}Ca_{0.3}TiO_3$ (BCT) and $Ba(Zr_{0.2}Ti_{0.8})O_3$ (BZT) xerogels and films is investigated and compared to that of BT and BZT–BCT. We analysed BCT and BZT xerogels by thermogravimetry, differential thermal analysis, and evolved gas analysis, and the as-deposited films by Fourier transform infrared (FTIR) spectroscopy. The crystallinity and microstructure of the films are reported.

2. Experimental part

$(Ba_{0.7}Ca_{0.3})TiO_3$ (BCT), and $Ba(Ti_{0.8}Zr_{0.2})O_3$ (BZT) coating solutions were prepared following the established procedure for BT published previously.[7] BCT coating solution is prepared using barium acetate $(Ba(CH_3COO)_2$ with a purity of 99.97% from Sigma-Aldrich, St. Louis, Missouri, USA), calcium acetate $(Ca(CH_3COO)_2$, 99.999%, Alfa Aesar, Karlsruhe, Germany), and titanium *n*-butoxide $(Ti(OC_4H_9)_4$, with a purity of 99.61% from Alfa Aesar, Karlsruhe, Germany) as precursors. The barium and calcium acetates are dissolved together in ethylene glycol ($HOCH_2CH_2OH$, EG, with a purity of 99.8% from Sigma-Aldrich, St. Louis, Missouri, USA) at room temperature in a conical flask. At the same time, the titanium n-butoxide is diluted in absolute ethanol (CH_3CH_2OH, EtOH, with a purity of 99.9% from Sigma-Aldrich, St. Louis, Missouri, USA) under a nitrogen atmosphere in a round flask. Both acetates and titanium solutions are then mixed at room temperature for 2 hours. The concentration of the solution is adjusted to 0.1 M for BCT films deposition.

The BZT coating solution was prepared following the same procedure, using zirconium n-butoxide $(Zr(OC_4H_9)_4$, $Zr(OnBu)_4$), 80% purchased from Alfa Aesar, Karlsruhe, Germany, and the above-mentioned $Ba(CH_3COO)_2$ and $Ti(OC_4H_9)_4$. Titanium and zirconium alkoxides are diluted with ethanol together in a round flask under a nitrogen atmosphere before adding the completely dissolved barium acetate in ethylene glycol. The concentration of the solution is adjusted to 0.1 M for BZT film deposition.

For the thermal analysis, BCT and BZT xerogels were obtained by drying the respective solutions at 200 °C for 12 hours. The thermal analysis of the xerogels was performed using a thermal analyzer coupled with a mass spectrometer (STA 409, Netzsch + ThermoStar, Balzers Instruments). The thermogravimetric curve (TG), differential thermal analysis (DTA), and evolved gas analysis (EGA) of both BCT and BZT samples using 40.5 mg and 34.6 mg of the respective xerogels in Pt/Rh crucibles were recorded at a heating rate of 10 °C/min in a flowing synthetic air atmosphere from room temperature up to 1200 °C.

Single-layer films of both BCT and BZT were deposited on $Pt(111)/TiO_2/SiO_2/Si(100)$ substrates (Pt/Si, purchased from SINTEF, Oslo, Norway) by spin coating at 3000 rpm for 30 seconds. The films were dried at 250 °C for 15 minutes and pyrolyzed at 350 °C for 15 minutes on hot plates. FTIR analysis was performed after the pyrolysis step and after each temperature increase during rapid thermal annealing (RTA) in the Mila 5000 furnace (Ulvac-Riko, Yokohama, Japan), with a heating rate of 13.3 °C per second between 400 °C and 750 °C, and hold times of 6 seconds at each temperature increase step until the full decomposition of organic residue. After pyrolysis, the temperature was increased in 100 °C steps to 500 °C, then in 50 °C steps until the full decomposition of carbon residues was achieved. The FTIR spectra were recorded using Attenuated Total Reflectance-Fourier Transform Infrared spectroscopy (Perkin Elmer ATR-FTIR Spectrum 100, 4000–380 cm^{-1}). The purpose of the FTIR analysis of the single-layer films was to study the decomposition of organics, the formation of carbonates, and their subsequent decomposition.

The BCT and BZT films were deposited by spin coating the 0.1 M coating solutions onto Pt/Si substrates at 3000 rpm for 30 seconds. The as-deposited films were dried at 250 °C for 15 minutes, pyrolyzed at 350 °C for 15

minutes on hot plates, and then annealed at 850 °C in a rapid thermal annealing furnace with a heating rate of 13.3 °C per second. The first and last layers were annealed for 15 minutes, while the intermediate layers were annealed for 5 minutes. The films consisted of ten deposited layers.

The XRD diffraction patterns of the crystalline samples were recorded using a high-resolution diffractometer (X'Pert PRO, PANalytical, Almelo, The Netherlands, Cu Kα radiation) in the following conditions: 2θ = 10–39°, 40–65 °, step = 0.034°, time per step = 100 seconds, Soller slit = 0.02, mask10. The recorded data were analysis using X'Pert High Score Plus software.

Scanning electron microscopy (SEM) was used to analyse the surface microstructure and cross-section of the films using a field-emission SEM Verios 4G HP (Thermo Fisher, Waltham, Massachusetts, USA).

3. Results and Discussion

BZT and BCT xerogels were prepared by drying the respective coating solutions at 200 °C to constant mass. The thermal decomposition of the xerogels was monitored by thermogravimetry (TG), differential thermal analysis (DTA), and evolved gas analysis (EGA). The recorded data were thoroughly analyzed.

The TG, DTA, and EGA curves recorded during the thermal decomposition of the BCT xerogel from room temperature to 1200 °C are shown in Figure 1. On the TG curve, the total mass loss of the sample during heating from room temperature to 780 °C is 39%. During heating to 200 °C, the mass loss is approximately 3%, coinciding with a slight endothermic peak on the DTA curve, attributed to the evaporation of residual solvent and/or adsorbed moisture. This is confirmed by the detection of H_2O on the EGA curve in the same temperature range. From 220 °C to 490 °C, the mass loss is approximately 23%, accompanied by strong exothermic peaks on the DTA curve at 300 °C, 340 °C, and 488 °C. The evolution of H_2O, CO_2, and acetone (CH_3COCH_3) is recorded by EGA, indicating the thermal oxidation of organic groups. CH_3COCH_3 is a side product of the thermal oxidation of the acetate to the oxide via the carbonate as an intermediate product.[21,22] In BT xerogels prepared using the same procedure, CH_3COCH_3 was detected only at approximately 400 °C.[7] In BCT, two CH_3COCH_3 peaks are recorded, one with a higher intensi-

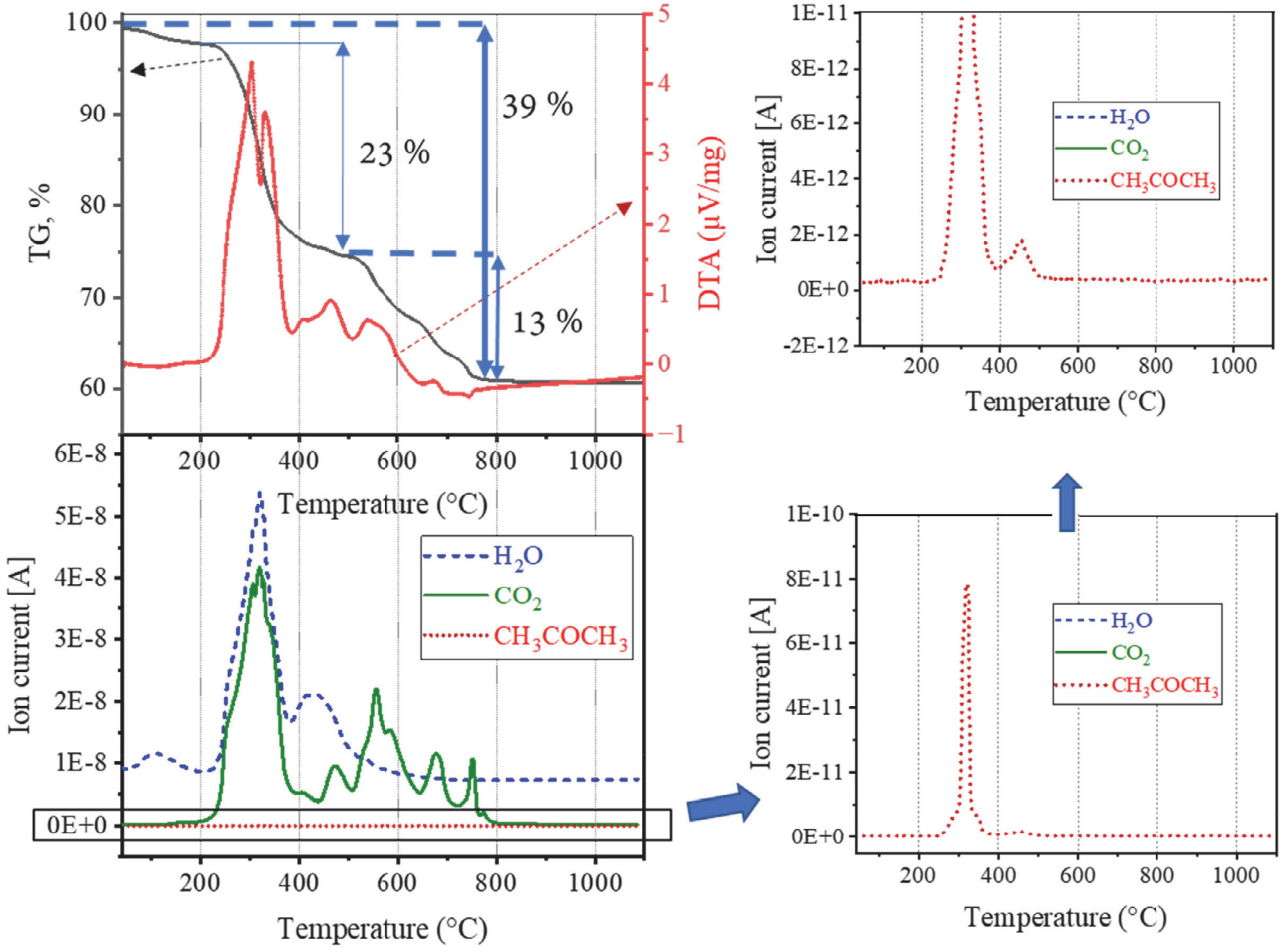

Figure 1. Thermal analysis: TG, DTA, and EGA curves of the BCT xerogel recorded from room temperature to 1200 °C.

ty at around 300 °C and the second, lower one at about 420 °C. The first peak is attributed to the decomposition of $Ca(CH_3COO)_2$, and the second peak to the decomposition of $Ba(CH_3COO)_2$. This indicates that the acetates do not decompose simultaneously; consequently, the respective carbonates would form at different temperatures.

Upon heating from 490 °C to 780 °C, the sample loses approximately 13% of its mass, which coincides with a series of exothermic peaks on the DTA curve and the detection of CO_2 peaks without H_2O, indicating thermal decomposition of carbonate groups. Upon heating to 1200 °C, the mass of the sample remains unchanged.

On the other hand, the final mass loss of the BZT xerogel occurs at a temperature of approximately 720 °C, which is 60 °C lower than that of BCT at 780 °C. The total mass loss of the BZT sample is approximately 33%, as shown in Figure 2. Similar to the BCT sample, upon heating from room temperature to 200 °C, the mass loss is approximately 4%, which coincides with a slight endothermic deflection of the DTA curve and the detection of H_2O in the EGA curve at 120 °C, which is attributed to the evaporation of residual solvent and/or adsorbed moisture. From approximately 250 °C to ≈720 °C, the sample loses 29% of its mass, coinciding with a series of exothermic peaks on the DTA curve at 390 °C, 460 °C, and 570 °C. The evolution of H_2O, CO_2, and CH_3COCH_3 is also recorded in this temperature range. This mass loss is attributed to the thermal oxidation of the functional groups. Note that the peak of CH_3COCH_3 around 300 °C is not recorded in BZT, thus confirming that it is the fingerprint of the $Ca(CH_3COO)_2$ decomposition in the BCT sample. The progressive mass loss of the BZT sample upon heating from 500 °C to 720 °C is accompanied by an exothermic DTA peak and the evolution of CO_2 due to the decomposition of carbonate groups.

The thermal decomposition of BT and BZT–BCT xerogels previously prepared using the same procedure and the same combination of reagents and solvents was concluded at 719 °C and 775 °C, respectively.[4,7] We observe that the thermal decomposition of BT and BZT xerogels is concluded at about 720 °C, and at about 60 °C higher temperature, at 780 °C, in BCT and BZT–BCT xerogels. We can therefore attribute the temperature increase of the thermal decomposition of BCT and BZT–BCT to $Ca(CH_3COO)_2$.

FTIR analysis of single-layer films was performed to support the thermal analysis and further investigate the formation of carbonate groups and their subsequent de-

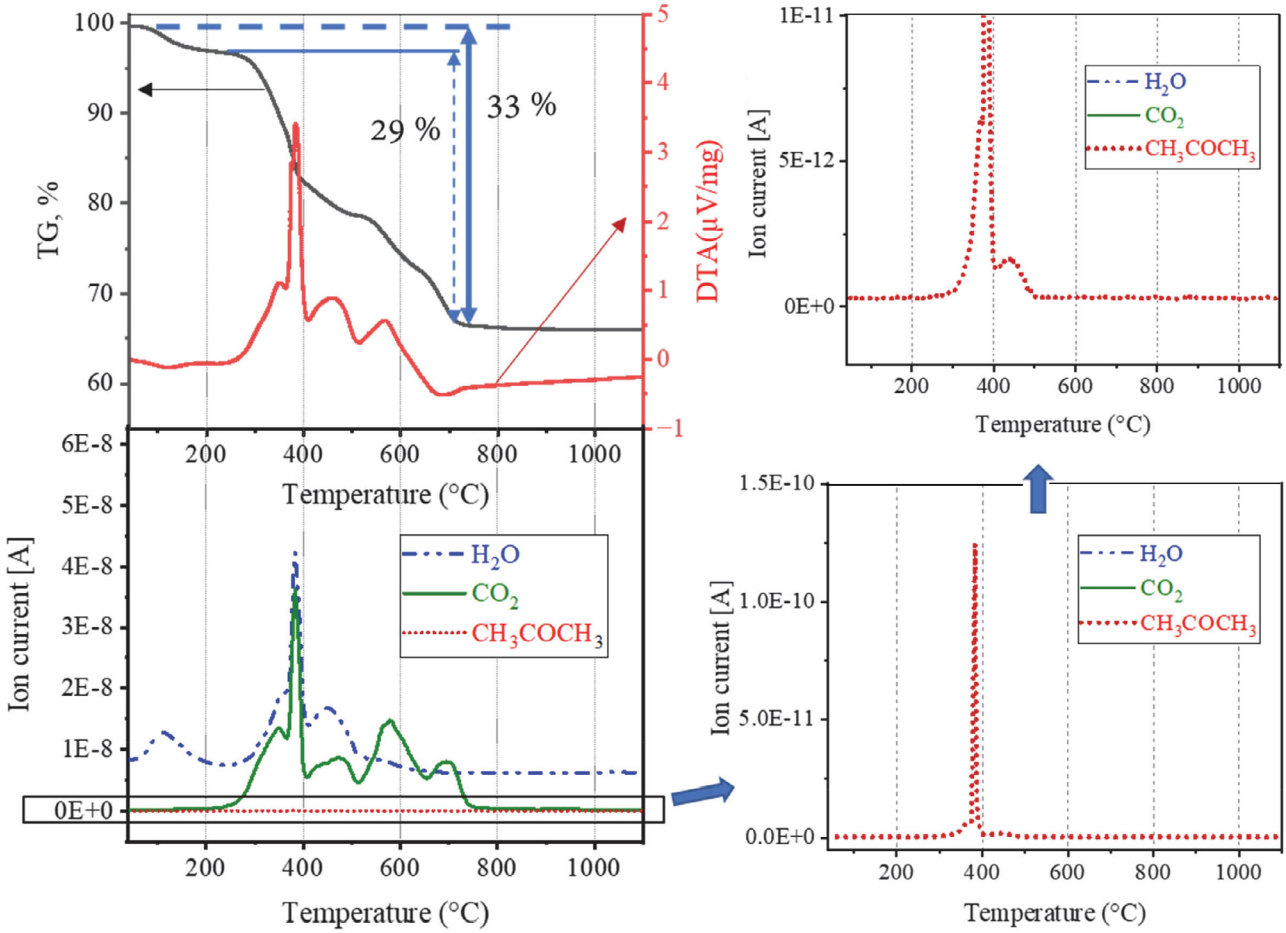

Figure 2. Thermal analysis: TG, DTA, and EGA curves of the BZT xerogels recorded from room temperature to 1200 °C.

composition. Note that the estimated thickness of the single-layer films was about 10 nm. The single-layer BCT and BZT film samples were dried at 250 °C and pyrolyzed at 350 °C on a hot plate. The FTIR spectra were recorded at temperatures ranging from 350 °C to 700 °C or 750 °C in 50 °C or 100 °C increments.

In the spectra of the films heated to 350 °C and 400 °C, absorption bands appear at 1563 cm^{-1} and 1463 cm^{-1}, as shown in Figure 3, characteristic of the symmetric and asymmetric vibrations of the acetate group (COO), and at 866 cm^{-1}, characteristic of the C–O bond.[6,23] The broad, indistinct absorption band below 800 cm^{-1} is attributed to vibrations of the Ti–O and Zr–O bonds, which form after decomposition of the alkoxide precursors.[4]

After heating the BCT film to 500 °C, the carboxylate group bands persist in the spectrum, suggesting that the carboxylate groups are not completely decomposed at 500 °C. The carbonate group absorption band is pronounced in the films heated between 600 °C and 700 °C, and disappears only after the film is heated to 750 °C, see Figure 3a). At this temperature, only the characteristic metal–oxygen bond bands are observed.

In contrast, in BZT, the carbonate group band is present in the FTIR spectra upon heating to 650 °C. In the spectrum of the sample heated at 700 °C, only pronounced absorption bands at 704 cm^{-1} and 452 cm^{-1}, characteristic of the Ti–O/Zr–O and Ba–O bonds, are observed, see Figure 3b).

In the FTIR spectra of the single-layer BZT and BCT films, carboxylate groups are present upon heating to temperatures from 350 °C to 500 °C, while carbonate groups are detected at higher temperatures. The latter groups decompose at 700 °C in the BZT film, and at 750 °C in BCT, which is 50 °C higher. A similar trend of upshifting the thermal decomposition temperature is observed in BT and BZT–BCT thin films prepared with the same solution chemistry. In BT and BZT–BCT thin films, the thermal decomposition of the carbonate groups is concluded at about 600 °C and above 750 °C, respectively.[4,7]

The FTIR analysis of the samples confirms the thermal analysis data, revealing that the thermal oxidation of BCT occurs at a higher temperature than that of BZT. It should be noted that, in BT films, the thermal oxidation of carbonate groups was concluded at 100 °C (BZT) and 150 °C (BCT) lower temperatures. According to literature, in solution-derived BT thin films, the perovskite phase crystallizes through an intermediate $Ba_2Ti_2O_5CO_3$ oxycarbonate phase[24] following Eq. 1.

$$Ba_2Ti_2O_5CO_3 \longrightarrow 2BaTiO_3 + CO_2 \qquad (1)$$

Similarly, we assume that in the presence of Ca-species, the perovskite would be formed via an intermediate bimetallic oxycarbonate $(Ba,Ca)_2Ti_2O_5CO_3$ phase or, possibly, a mixture of single-alkaline-earth metal oxycarbonates, $Ca_2Ti_2O_5CO_3$ and $Ba_2Ti_2O_5CO_3$, which may require higher thermal energy for the decomposition of the carbonate groups and the perovskite crystallization than Ba-Ti-oxycarbonate. We may assume a similar situation in the case of BZT, namely the formation of a mixed $Ba_2(Ti,Zr)_2O_5CO_3$ intermediate phase or a mixture of $Ba_2Ti_2O_5CO_3$ and $Ba_2Zr_2O_5CO_3$. Two or more different

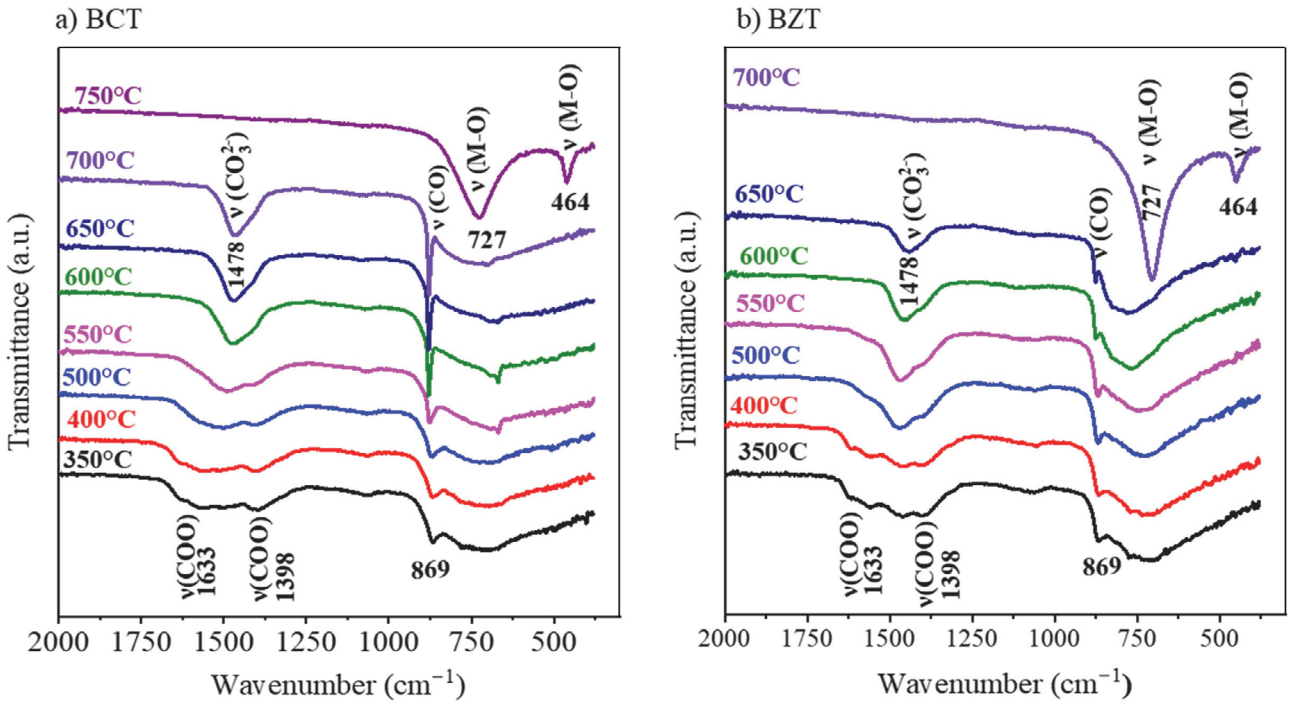

Figure 3. FTIR of single-layer a) BCT and b) BZT films after heating to different temperatures

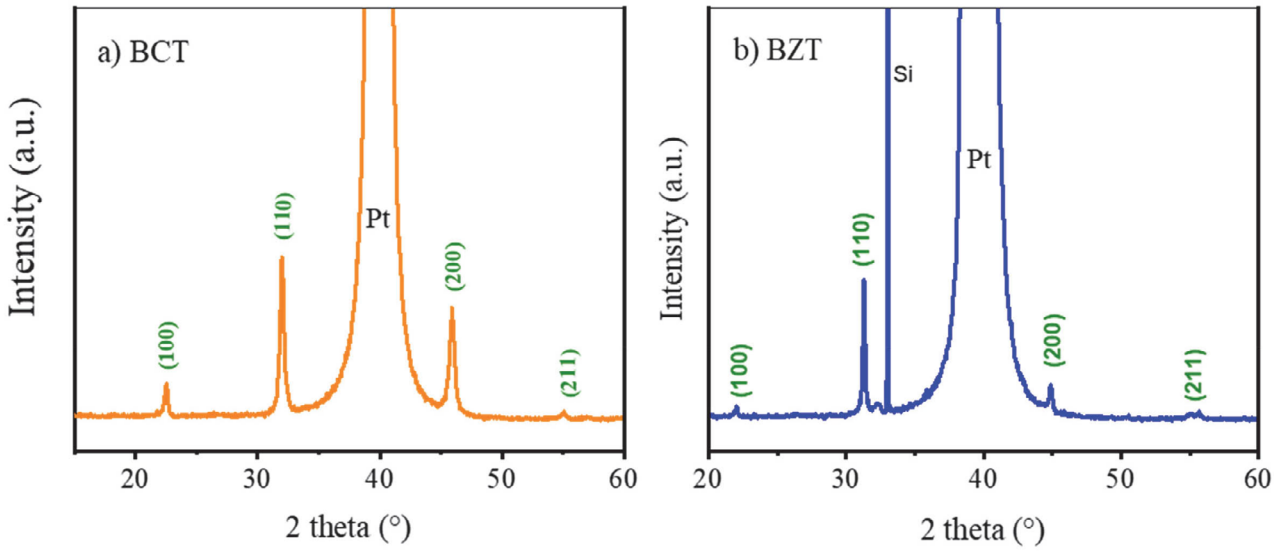

Figure 4. XRD patterns of a) BCT and b) BZT thin films. The perovskite phase peaks are indexed according to PDF-01-074-4539 (cubic $BaTiO_3$).

oxycarbonates may upshift the decomposition temperature of organic residues, and subsequently the crystallization of the perovskite phase and the densification of the thin film.

Figure 4 shows the XRD patterns of BCT and BZT thin films prepared by repeated deposition-drying-pyrolysis-annealing at 850 °C. Both samples crystallize in the perovskite phase (PDF-01-074-4539), with the strongest diffraction peak being (110) in both cases. In both films, Pt (111) peak of the substrate coincides with the (111) perovskite peak; therefore, we cannot quantify the crystalline orientation of the films.

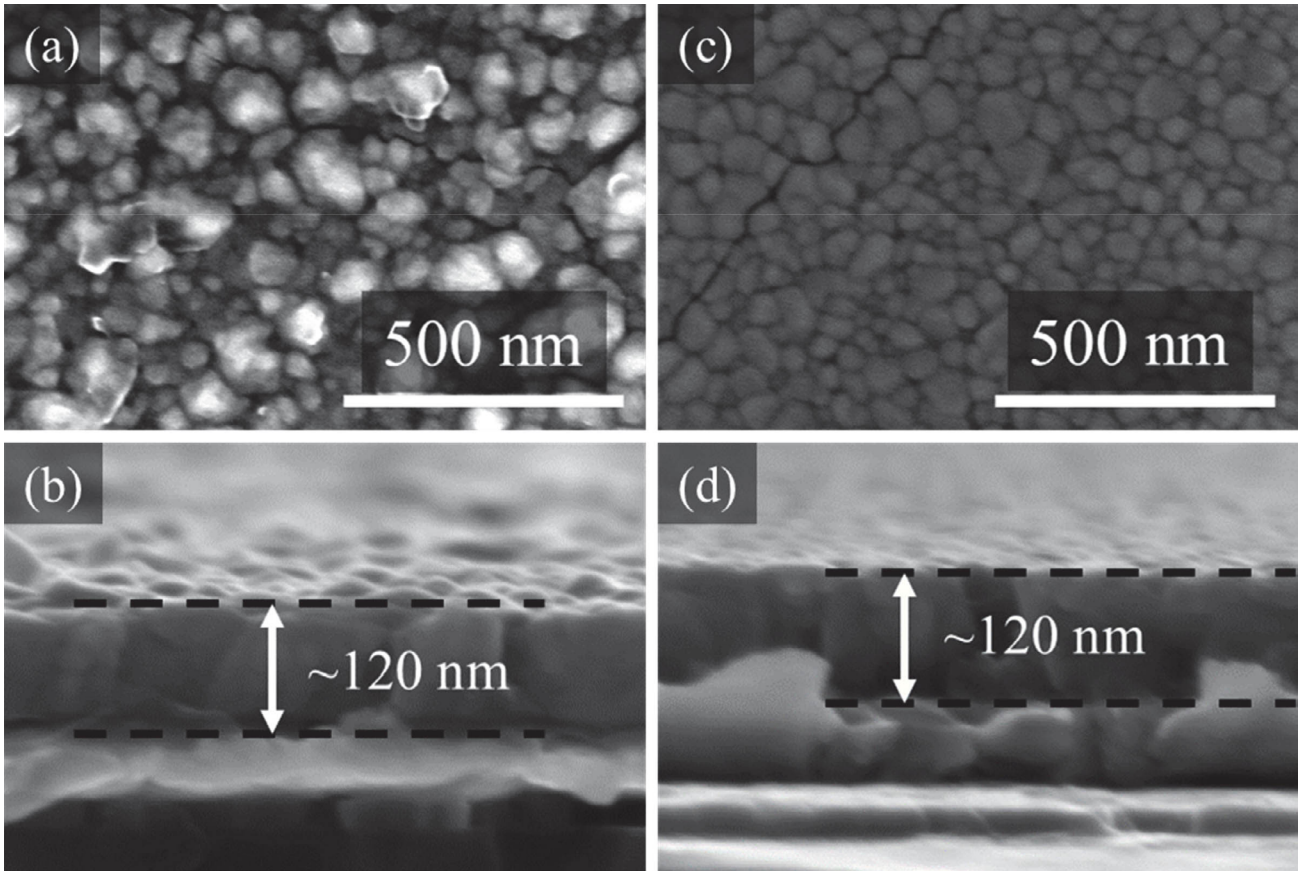

Figure 5. SEM plan view of: (a) BCT and (c) BZT thin films and their respective cross-section (b) and (d).

Figure 5 shows the surface and cross-section microstructures of BCT and BZT films. From the cross-sectional images, the film thickness is approximately 120 nm. The surface microstructure of both films is dense and consists of grains a few tens of nanometers across. Intergranular cracks are observed on both surfaces, the origin of which was previously related to thermal stresses developed in the BZT–BCT film as a consequence of the thermal expansion mismatch between the film and the substrate.[25,26] We expect that the thermal expansion coefficients of BCT and BZT would be close to those of BZT–BCT.

4. Conclusion

$(Ba_{0.7}Ca_{0.3})TiO_3$ (BCT) and $Ba(Zr_{0.2}Ti_{0.8})O_3$ (BZT) are end members of the BZT–BCT solid solution, which exhibits excellent piezoelectric properties at the equimolar BZT/BCT ratio and is a strong lead-free candidate to replace lead-based piezoelectric ceramic materials. The study provides a detailed insight into the decomposition pathways of xerogels obtained from coating solutions for BCT and BZT thin films, as analyzed by thermal analysis and Fourier transform infrared spectroscopy. The carbonate residues formed from BCT and BZT xerogels are fully decomposed upon heating to 780 °C and 720 °C, respectively. The thermal decomposition of the carbonate residues in BCT and BZT thin films is concluded at 750 °C and 700 °C, respectively. The thermal analysis of xerogels and FTIR spectroscopy of the films indicate that Ca-species, most probably Ca-oxycarbonate, contribute to the increase in the decomposition temperature of carbonate residues in BCT xerogels and thin films compared to BZT. BCT and BZT films annealed at 850 °C crystallize in the perovskite phase. The microstructure of the films is characterized by a grain size of a few tens of nanometers.

Acknowledgements

The authors acknowledge the financial support from the Slovenian Research and Innovation Agency (core funding P2-0105, young researcher projects of SWK and KŽ).

5. References

1. E. Wainer, *Trans. Electrochem. Soc.* **1946**, *89*, 331–356. **DOI:**10.1149/1.3071718
2. H. Han, J. Wang, Z. Wang, C. Liu, B. Xiang, *Appl. Opt.* **2023**, *62*, 6053–6059. **DOI:**10.1364/AO.499065
3. J. Y. Hsu, J. Y. M. Lee, J. J. Wang, L. Y. Yeh, J. T. Lai, J. Gong, *International Electron Devices and Materials Symposium, IEEE.* **1994**, 11-32-128-11-32–131.
4. S. W. Konsago, K. Žiberna, J. Ekar, J. Kovač, B. Malič, *J. Mater. Chem. C* **2024**, *12*, 14658–14666. **DOI:**10.1039/D4TC02495H
5. S. Hoffmann, R. Waser, *J. Eur. Ceram. Soc*. **1999**, *19*, 1339–1343. **DOI:**10.1016/S0955-2219(98)00430-0
6. U. Hasenkox, S. Hoffmann, R. Waser, *J. Sol-gel Sci. Technol.* **1998**, *12*, 67–79. **DOI:**10.1023/A:1026480027046
7. S. W. Konsago, K. Žiberna, B. Kmet, A. Benčan, H. Uršič, B. Malič, *Molecules* **2022**, *27*, 3753 (1–17). **DOI:**10.3390/molecules27123753
8. W. Liu, X. Ren, *Phys. Rev. Lett*. **2009**, *103*, 257602. **DOI:**10.1103/PhysRevLett.103.257602
9. M. McQuarrie, F. W. Behnke, *J. Am. Ceram. Soc*. **1954**, *37*, 539–543. **DOI:**10.1111/j.1151-2916.1954.tb13986.x
10. L. Liu, S. Ren, J. Zhang, B. Peng, L. Fang, D. Wang, *J. Am. Ceram. Soc*. **2018**, *101*, 2408–2416. **DOI:**10.1111/jace.15410
11. H. Tsukasaki, Y. Inoue, Y. Koyama, *Mater. Sci. Forum* **2014**, *783–786*, 2400–2405. **DOI:**10.4028/www.scientific.net/MSF.783-786.2400
12. J. F. Ihlefeld, J.-P. Maria, W. Borland, *J. Mater. Res.* **2005**, *20*, 2838–2844. **DOI:**10.1557/JMR.2005.0342
13. Q. Jia, B. Shen, X. Hao, S. Song, J. Zhai, *Mater. Lett.* **2009**, *63*, 464–466. **DOI:**10.1016/j.matlet.2008.11.026
14. B. Singh, S. Kumar, G. S. Arya, N. S. Negi, *AIP Conference Proceedings* **2015**, 060005-1 - 060005-5. **DOI:**10.1063/1.4915375
15. J. Zhai, X. Yao, J. Shen, L. Zhang, H. Chen, *J. Phys. D Appl. Phys.* **2004**, 37, 748–752. **DOI:**10.1088/0022-3727/37/5/016
16. T. Ohno, K. Uchida, N. Sakamoto, D. Fu, N. Wakiya, T. Matsuda, H. Suzuki, *Jpn. J. Appl. Phys.* **2010,** *49*, 09MA11. **DOI:**10.1143/JJAP.49.09MA11
17. H. T. Vu, H. N. Vu, G. Rijnders, M. D. Nguyen, *J. Alloys. Compd*. **2023**, *968,* 171837. **DOI:**10.1016/j.jallcom.2023.171837
18. X. Yan, K. H. Lam, X. Li, R. Chen, W. Ren, X. Ren, Q. Zhou, K. K. Shung, *IEEE Trans. Ultrason. Ferroelectr. Freq. Control.* **2013**, *60*, 1272–1276. **DOI:**10.1109/TUFFC.2013.2692
19. J. Gao, D. Xue, W. Liu, C. Zhou, X. Ren, *Actuators* **2017**, *6*, 1–20. **DOI:**10.3390/act6030024
20. S. W. Konsago, K. Žiberna, A. Matavž, B. Mandal, S. Glinšek, Y. Fleming, A. Bencan, G. L. Brennecka, H, Uršič, B. Malič, *ACS Appl. Electron. Mater*. **2024**, *6,* 4467–4477.
21. B. Malic, M. L. Calzada, J. Cilensek, L. Pardo, M. Kosec, *Adv. Appl. Ceram*. **2010**, *109,* 147–151. **DOI:**10.1179/174367509X12502621261415
22. B. Malič, M. Kosec, K. Smolej, S. Stavber, *J. Eur. Ceram. Soc.* **1999**, *19*, 1345–1348. **DOI:**10.1016/S0955-2219(98)00431-2
23. L. Fè, G. Norga, D. J. Wouters, R. Nouwen, L. C. Van Poucke, *J. Sol-gel Sci. Technol.* **2000**, *19,* 149–152. **DOI:**10.1023/A:1008707531737
24. H. S. Gopalakrishnamurthy, M. Subba Rao, T. R. Narayanan Kutty, *J. Inorg. Nucl. Chem.* **1975**, *37*, 891–898. **DOI:**10.1016/0022-1902(75)80668-3
25. S. W. Konsago, A. Debevec, J. Cilenšek, B. Kmet, B. Malič, *Informacije MIDEM.* **2023**, *53*, 233–238.
26. W. M. Yim, R. J. Paff, *J. Appl. Phys*. **1974**, *45,* 1456–1457. **DOI:**10.1063/1.1663432

Povzetek

Razumevanje termičnega razpada in kristalizacije perovskitne faze omogoča načrtovanje mikrostrukture tankih plasti na osnovi $BaTiO_3$, pripravljenih s sintezo v raztopini. Iz raztopin prekurzorjev $(Ba_{0.7}Ca_{0.3})TiO_3$ (BCT) in $Ba(Zr_{0.2}Ti_{0.8})O_3$ (BZT) smo pripravili ustrezna kserogela s sušenjem pri 200 °C in tanke plasti BCT in BZT z nanašanjem na podlage z metodo vrtenja. Termični razpad organskih skupin v kserogelih poteče preko oksikarbonatnih skupin, ki razpadejo šele po segrevanju pri temperaturah 780 °C (BCT) oziroma 720 °C (BZT). V tankih plasteh BCT in BZT po segrevanju pri 750 °C oziroma 700 °C na zaznamo več sledov ogljikovih faz. Približno 120 nm debele plasti BCT in BZT kristalizirajo v perovskitni fazi po segrevanju pri 850 °C.